# AMP-activated protein kinase activator, HL156A reduces thioacetamide-induced liver fibrosis in mice and inhibits the activation of cultured hepatic stellate cells and macrophages

HYE SHIN LEE[1], HYUN-SANG SHIN[1], JINHYEOK CHOI[1], SUNG-JIN BAE[1], HEE-JUN WEE[1], TAEKWON SON[1], JI HAE SEO[1], JI-HYEON PARK[1], SUNG-WUK KIM[3] and KYU-WON KIM[1,2]

[1]SNU-Harvard NeuroVascular Protection Research Center, College of Pharmacy and Research Institute of Pharmaceutical Sciences, Seoul National University, Seoul 08826; [2]Crop Biotechnology Institute, GreenBio Science and Technology, Seoul National University, Pyeongchang 25354; [3]Hanall Biopharma Co. Ltd., Seoul 16170, Republic of Korea

Received April 8, 2016; Accepted May 4, 2016

DOI: 10.3892/ijo.2016.3627

**Abstract.** Cirrhosis, the end-stage of hepatic fibrosis, is not only life-threatening by itself, but also a causative factor of liver cancer. Despite efforts to develop treatment for liver fibrosis, there are no approved agents as anti-fibrotic drugs to date. In the present study, we aimed to investigate the anti-fibrotic effect of the AMP-activated protein kinase (AMPK) activator, HL156A. A mouse model of thioacetamide (TAA)-induced liver fibrosis was used to examine the effect of HL156A *in vivo*. Mice received either TAA alone or a combination of TAA and HL156A intraperitoneally for a total duration of 6 weeks. Including HL156A during exposure to TAA significantly reduced extracellular matrix (ECM) deposition and production of the hepatic transforming growth factor-β1 (TGF-β1). Immunohistochemical analysis revealed that the activation of hepatic stellate cells and the capillarization of liver sinusoids were also diminished significantly by HL156A co-treatment. The anti-fibrotic effect of HL156A was further studied *in vitro* by using a rat hepatic stellate cell line, HSC-T6 cells. The induction of α-smooth muscle actin (α-SMA) by TGF-β1 treatment was reversed by HL156A, which was likely via the activation of AMPK. Moreover, HL156A showed anti-inflammatory effects on macrophages. Treatment with HL156A diminished LPS-induced activation of both Raw264.7 macrophage cells and primary cultured mouse macrophages. Taken together, these results imply that the AMPK activator HL156A inhibits hepatic fibrosis via multiple mechanisms and could be a potentially effective agent for fibrosis treatment.

*Correspondence to:* Dr Kyu-Won Kim, SNU-Harvard Neuro-Vascular Protection Research Center, College of Pharmacy and Research Institute of Pharmaceutical Sciences, Seoul National University, Seoul 08826, Republic of Korea
E-mail: qwonkim@snu.ac.kr

*Key words:* liver fibrosis, HL156A, AMP-activated protein kinase, hepatic stellate cells, macrophages

## Introduction

Hepatic fibrosis is the wound healing response of the liver to chronic hepatic injury caused by virus infection, alcohol ingestion and biliary dysfunction. Several studies have elucidated the various types of effector cells involved in fibrogenesis and molecular mechanisms regulating these effector cells (1-3). Hepatic stellate cells (HSCs) are generally considered as the most prominent cell type involved in liver fibrogenesis. These cells, upon myofibroblastic transition (or activation) in response to fibrogenic stimuli, produce large amounts of ECM proteins, which in turn lead to increased stiffness of the liver (4).

Although HSC is recognized as a major player in liver fibrosis, its myofibroblastic transition is regulated by multiple factors such as inflammation and vascular remodeling. In the initial stage of fibrogenesis, injured hepatocytes elicit an inflammatory response that initiates pro-fibrotic cascades (3,5). For example, infiltrated macrophages release not only pro-inflammatory cytokines such as tumor necrosis factor (TNF)-α, interleukin (IL)-6, and IL-1β, but also generate pro-fibrotic growth factors such as TGF-β1 and platelet-derived growth factor (PDGF). At the same time, liver sinusoidal endothelial cells (LSECs) undergo vascular remodeling under fibrogenic conditions. The vascular remodeling includes angiogenesis as well as 'capillarization' in which LSECs start to have a basement membrane typical to capillaries in other organs. Such vascular remodeling is known to make LSECs lose their normal function of inhibiting HSC activation, which in turn, promotes fibrosis (6-8).

AMPK is a cellular sensor of energy metabolism that maintains energy homeostasis of the cell (9). Since many human disorders including type 2 diabetes, cancer, and inflammatory disease are related to impaired energy balance, AMPK is becoming a promising drug target for a wide range of diseases (10-12). Several lines of studies also reported the importance of AMPK signaling in hepatic fibrosis. For instance, some AMPK activators such as 5-aminoimidazole-4-carboxamide ribonucleotide (AICAR), metformin, and berberine have shown anti-fibrotic effects in animal models of

liver fibrosis (13,14) and inhibit TGF-β1-induced activation of cultured HSCs (15). Moreover, activation of AMPK prevents the activation of macrophages in culture (16) and inhibits inflammation either in liver or in adipose tissues (16,17). Therefore, AMPK signaling is unlikely to target a single cell type; rather, it affects multiple cell types.

HL156A is a novel derivative of phenyl biguanide that is capable of inducing AMPK phosphorylation more potently than metformin or AICAR (18). Recently, HL156A has been reported to possess anti-fibrotic activity in an animal model of peritoneal fibrosis (18). Based on the recent finding on the HL156A effects on peritoneal fibrosis and the importance of AMPK signaling in liver fibrogenesis, we hypothesized that HL156A may have therapeutic potential for liver fibrosis. In the present study, we therefore explored the anti-fibrotic effect of HL156A in a mouse model of TAA-induced liver fibrosis as well as in cultured HSCs and macrophages.

## Materials and methods

*Animal treatment*. All animal procedures conducted in this study were approved by the Committee for Care and Use of Laboratory Animals at Seoul National University, according to the Guide for Animal Experiments edited by the Korean Academy for Medical Sciences. Male 8-week-old C57BL/6 mice were purchased from Orient Bio (Seoul, Korea). The mice were randomly assigned to four groups. The vehicle group (n=4) received saline, and the TAA group (n=4) received thioacetamide intraperitoneally three times a week for a total duration of 6 weeks. The injection doses of TAA (Sigma-Aldrich, St. Louis, MO, USA) were 50 mg/kg for the first injection, 100 mg/kg for the second injection and 150 mg/kg for third to sixth injections and 300 mg/kg for the rest of the injections. The TAA and HL156A co-treatment groups (n=5 each) received the same TAA as the TAA group and HL156A was intraperitoneally injected on the alternative days of TAA injection at a dose of either 2 mg/kg or 10 mg/kg. After 6 weeks of treatment, mice were euthanized via deep anesthesia followed by cardiac perfusion.

*Histological analysis and immunohistochemistry*. The paraffin sections were de-paraffinized and stained with hematoxyline and eosin (H&E) or Picro-Sirius Red (Abcam, Cambridge, MA, USA) according to manufacturer's instructions. Immunohistochemistry was performed as previously described (19). Briefly, paraffin sections were subjected to antigen retrieval by incubating in Tris-EDTA buffer (10 mM Tris Base, 1 mM EDTA, 0.05% Tween-20, pH 9.0) for 40 min at 95˚C. After blocking with 5% normal donkey serum (Sigma-Aldrich)/PBS solution, the sections were incubated overnight at 4˚C with primary antibodies for α-smooth muscle actin (α-SMA) (1:200, Dako, San Diego, CA, USA), Desmin (1:200, Abcam), and Laminin (1:200, Sigma). After extensive washing in PBS/0.1% Tween-20 solution, the sections were treated with Alexa-488 or 546-conjugated secondary antibodies (1:750, Invitrogen, Carlsbad, CA, USA) for 1 h at room temperature followed by counter staining with Hoechst (Sigma). Fluorescent images were taken under confocal microscope (Carl Zeiss AG, Oberkochen, Germany), and immuno-positive areas were quantified by ImageJ software.

Table I. Primer sequences used in this study.

| Primers | Sequences (5'→3') |
|---|---|
| *col1a1* (sense) | CATGTTCAGCTTTGTGGACCT |
| *col1a1* (antisense) | GCAGCTGACTTCAGGGATGT |
| *col3a1* (sense) | TCCCCTGGAATCTGTGAATC |
| *col3a1* (antisense) | TGAGTCGAATTGGGGAGAAT |
| *tgf-β1* (sense) | TTGCTTCAGCTCCACAGAGA |
| *tgf-β1* (antisense) | TGGTTGTAGAGGGCAAGGAC |
| *IL-6* (sense) | TTCCATCCAGTTGCCTTCTTG |
| *IL-6* (antisense) | GGGAGTGGTATCCTCTGTGAAGTC |
| *IL-1β* (sense) | CTACAGGCTCCGAGATGAACAAC |
| *IL-1β* (antisense) | TCCATTGAGGTGGAGAGCTTTC |
| *gapdh* (sense) | TGAACGGGAAGCTCACTGG |
| *gapdh* (antisense) | TCCACCACCCTGTTGCTGTA |

*Cell culture*. HSC-T6 cells were kindly provided by Dr Scott L. Friedman of Icahn School of Medicine at Mount Sinai. HSC-T6 cells were maintained in Dulbecco's modified Eagle's medium (DMEM; GenDEPOT, Barker, TX, USA) containing 10% fetal bovine serum (FBS, GenDEPOT), 100 U/ml penicillin and 100 μg/ml streptomycin (GenDEPOT). To investigate the effect of HL156A on HSC activation, cells were pre-treated with HL156A at indicated doses for 2 h and then treated with TGF-β1 (Peprotech, Rocky Hill, NJ, USA) for 16 h in serum-free condition. Raw264.7 cells were purchased from Korean Cell Line Bank (KCLB, Seoul, Korea) and maintained in DMEM containing 10% FBS, 100 U/ml penicillin, and 100 μg/ml streptomycin. The cells were pre-treated with HL156A for 2 h at indicated doses and with LPS (Sigma) for another 4 h. Primary macrophages were obtained from cultures of bone marrow cells from femora and tibiae of 6 to 8-week-old male C57BL/6 mice. In brief, mouse total bone marrow cells were isolated by flushing the diaphysis of femora and tibiae with cold PBS and incubating overnight in cell culture dishes in α-modified Eagle medium (α-MEM; Thermo Fisher Scientific, Waltham, MA, USA) supplemented with 10% FBS, to remove non-hematopoietic lineage cells. After discarding adherent cells, floating cells were further incubated in α-MEM supplemented with 10% FBS and macrophage colony-stimulating factor (M-CSF) (30 ng/ml, BioLegend, San Diego, CA, USA) in Petri dishes. After 6 days, non-adherent cells were removed and bone marrow macrophages (BMMs) were re-plated and used in the experiments.

*RNA extraction and RT-qPCR*. Liver tissues were incubated in Trizol Reagent (Invitrogen) for 5 min followed by homogenization using Tissue Lyser II (Qiagen, Hilden, Germany). Total RNA was isolated according to the manufacturer's instructions. Total RNA (2 μg) from each sample was reverse-transcribed with Moloney murine leukemia virus (MMLV) reverse transcriptase (Promega Corp., Madison, WI, USA). Quantitative real-time PCR was then performed using StepOnePlus real-time PCR system (Applied Biosystems, Foster city, CA, USA)

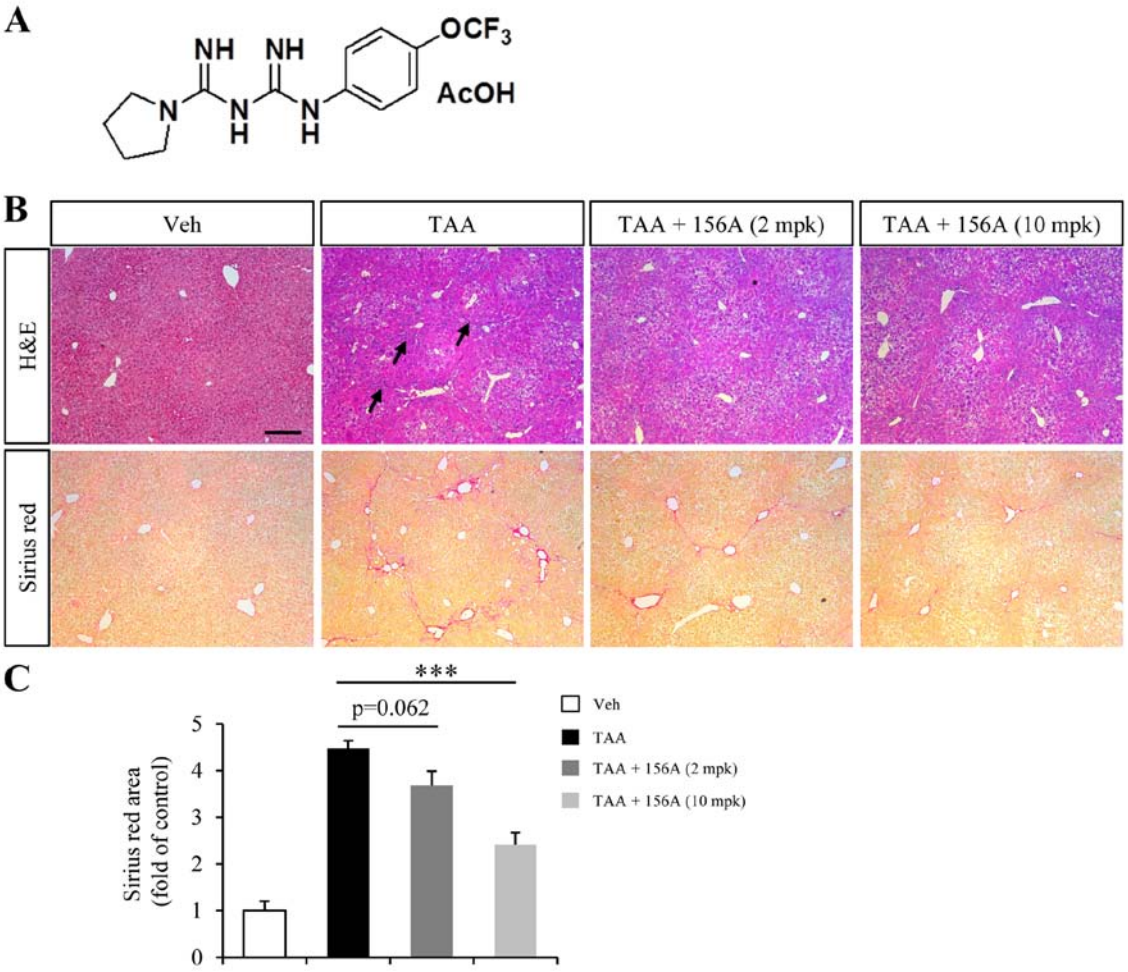


Figure 1. HL156A reduces liver fibrosis induced by TAA in mice. (A) Structure of HL156A. (B) Representative H&E (upper) and Sirius Red (lower) images of liver sections of four experimental mouse groups. Veh, vehicle; TAA, TAA alone; TAA+156A (2 mpk), co-administration of TAA and HL156A at a dose of 2 mg/kg; TAA+156A (10 mpk), co-administration of TAA and HL156A at a dose of 10 mg/kg each. Scale bar represents 200 $\mu$m. (C) Bar graph showing relative Sirius Red-positive area of each group [n=4 in Veh and TAA groups, n=5 in TAA+156A (2 mpk) and TAA+156A (10 mpk) groups]. Error bars represent SEM, $^{***}$P<0.001.

with RealHelix qPCR kit (NanoHelix, Seoul, Korea). The relative mRNA levels were normalized using glyceraldehyde 3-phosphate dehydrogenase (GAPDH) as an internal control. Primer sequences used for PCR are summarized in Table I.

*Western blotting.* Cells were lysed in radioimmunoprecipitation assay (RIPA) buffer containing 25 mM Tris pH 7.4, 150 mM NaCl, 5 mM $MgCl_2$, 0.5% NP-40, phosphatase inhibitor cocktail (Sigma) and proteinase inhibitor cocktail (Calbiochem, Billerica, MA, USA). Protein concentrations were determined using a bicinchoninic acid (BCA) Assay kit (Thermo). Lysates (20 to 30 $\mu$g) were resolved on polyacrylamide gel and then immunoblotted as previously described (20). The following antibodies were used; mouse anti-α-SMA (Dako, Glostrup, Denmark), rabbit anti-vinculin (Santa Cruz Biotechnology, Dallas, TX, USA), rabbit anti-phosphoAMPK Thr172 (Cell Signaling Technology, Beverly, MA, USA), and rabbit anti-phosphoSmad2 (Cell Signaling Technology).

*Nitric Oxide (NO) assay.* NO assay was carried out in Raw264.7 cells as previously described (20). In brief, sub-confluent cells were first treated with HL156A for 2 h and then incubated in the presence or absence of lipopolysaccharide (LPS) (100 ng/ml) for 24 h. The conditioned medium was then collected and mixed with the same volume of Griess reagent (1:1 mixture of 1% sulfanilamide in 30% acetate and 0.1% N-1-aphthylethylenediamine dihydrochloride in 60% acetate) at room temperature for 10 min. The absorbance of the incubated samples was measured by using microplate reader at 540 nm. The concentration of nitrite in each sample was calculated based on a standard curve built with known concentrations of sodium nitrite.

*Cell viability assay.* Cells were plated on 96-well plates and treated with serial doses of HL156A for 24 h to investigate its effect on cell viability. Relative cell viability was measured using CellTiter 96® AQueous One Solution Cell Proliferation Assay System (Promega Corp.) according to manufacturer's protocol.

*HL156A synthesis.* HL156A is a derivative of phenyl biguanide, which is designed and synthesized by Hanall Biopharma Inc. (Seoul, Korea). The detailed procedure of HL156A synthesis was described in a previous study (18).

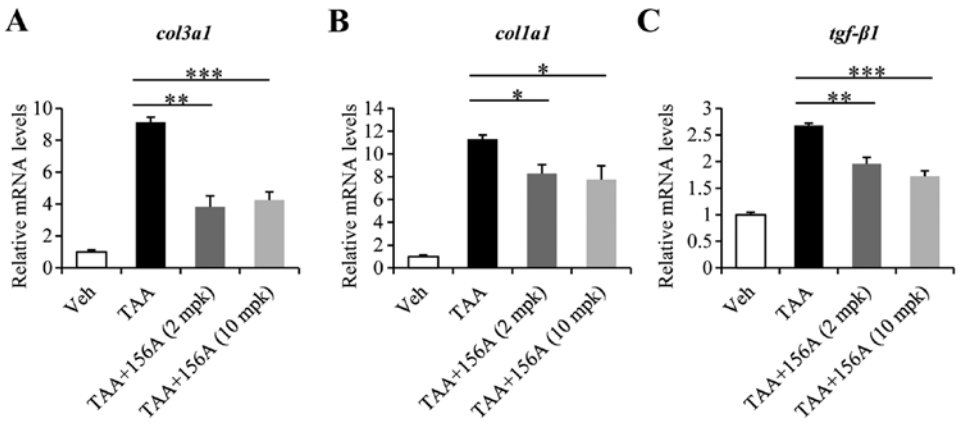


Figure 2. RT-qPCR of liver lysates showing decreases in ECM gene expression and a pro-fibrotic cytokine by HL156A. (A and B) Graphs showing relative mRNA levels of col3a1 (A) and col1a1 (B) in four experimental groups. (C) Graph showing relative mRNA levels of TGF-β1 in four experimental groups. Values are relative to veh control normalized by GAPDH levels [n=4 in Veh and TAA groups, n=5 in TAA+156A (2 mpk) and TAA+156A (10 mpk) groups]. Error bars represent SEM, $^{*}$P<0.05, $^{**}$P<0.01, $^{***}$P<0.001.

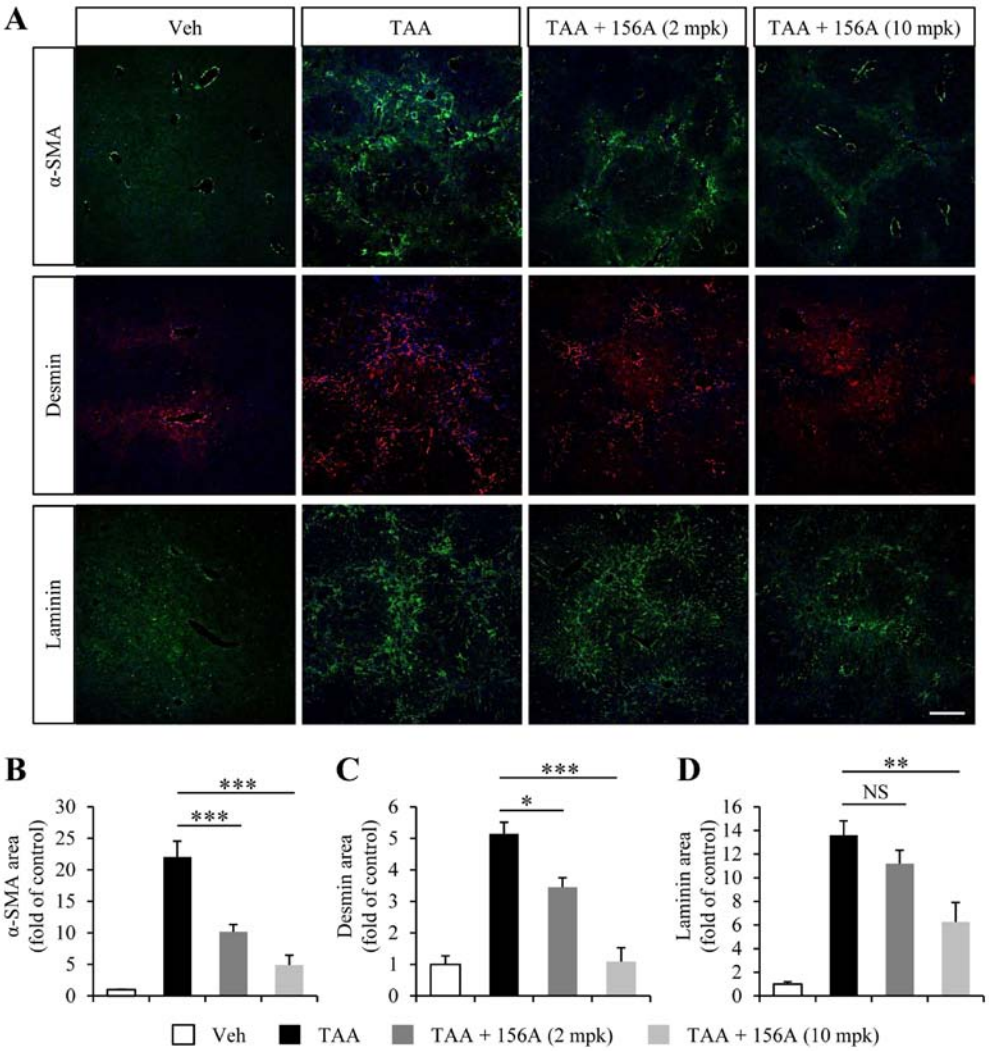


Figure 3. Immunohistochemical analysis of liver sections reveals reduced HSC activation and endothelial capillarization by HL156A. (A) Representative fluorescence images for α-SMA (green in upper row), desmin (red in middle row), and laminin (green in lower row) staining of liver sections. Scale bar represents 200 $\mu$m. Graphs showing relative areas positive for α-SMA (B), desmin (C) and laminin (D). Values are folds of Veh control (n=4 in Veh and TAA groups, n=5 in TAA+156A (2 mpk) and TAA+156A (10 mpk) groups). Error bars represent SEM, $^{*}$P<0.05, $^{**}$P<0.01, $^{***}$P<0.001; NS, not significant.

*Statistics*. Data were expressed as mean ± SEM. One-way ANOVA followed by Tukey's test or two-tailed Student's t-test was used for statistical analysis. Differences were considered significant at a P-value <0.05.

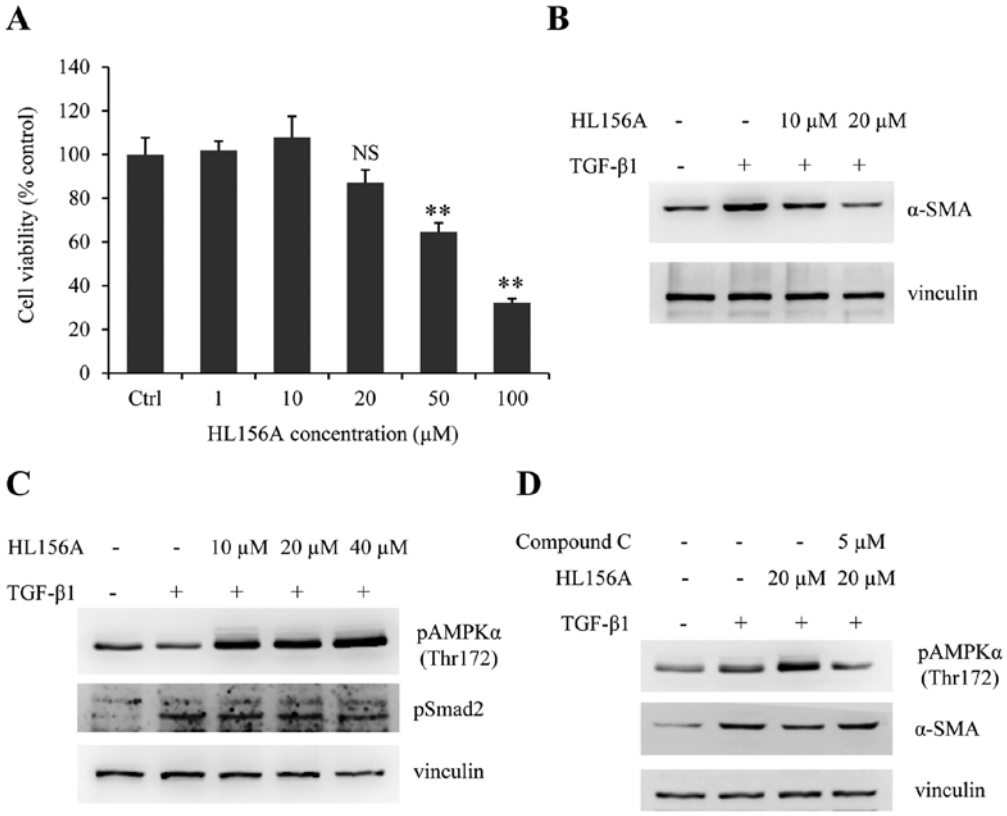


Figure 4. HL156A inhibits TGF-β1-induced α-SMA expression in HSCs via activation of the AMPK signaling. (A) HSC-T6 cells were cultured for 24 h in the presence of indicated concentrations of HL156A and relative cell viability was measured by MTS assay. Data are expressed as mean ± SEM (n=5). $^{**}$P<0.01 vs. control (ctrl); NS, not significant. (B) HSC-T6 cells were treated with TGF-β1 (10 ng/ml) alone or in combination with HL156A at indicated doses for 16 h. Note that HL156A reversed TGF-β1-induced α-SMA expression. (C) HSC-T6 cells were pre-treated with indicated amounts of HL156A for 2 h and TGF-β1 was added for 30 min. Western blotting shows increased phosphorylation of AMPKα by HL156A whereas TGF-β1-mediated Smad phosphorylation is unchanged. (D) HSC-T6 cells were treated with indicated combinations of reagents for 16 h. The AMPK inhibitor, compound C, abrogated effects of HL156A on both AMPK phosphorylation and α-SMA reduction. Western blot data are representatives of at least three independent experiments. Vinculin was used as a loading control.

## Results

*HL156A reduces TAA-induced liver fibrosis in mice*. TAA is one of the common hepatotoxins used in experimental liver fibrosis that causes centrilobular fibrosis (21). Since TAA-induced liver fibrosis is reversible by the withdrawal of TAA exposure, mice were treated with HL156A and TAA together to investigate the anti-fibrotic effect of HL156A in liver. Low (2 mg/kg) or high (10 mg/kg) dose of treatment was decided based on a previous study done in rodents (18). Repeated TAA injection for a total duration of 6 weeks resulted in inflammation and alteration of liver histology (Fig. 1B, arrows in upper row). Massive ECM deposition was also obvious in TAA group as revealed by Sirius Red staining (Fig. 1B, lower row). Co-treatment with low dose HL156A slightly reduced ECM deposition but the difference relative to TAA alone group was not statistically significant. High dose of HL156A, however, significantly reduced TAA-induced ECM deposition by approximately 40% when compared to TAA group (Fig. 1B and C).

*HL156A decreases mRNA levels of collagens and tgf-β1 induced by liver fibrosis*. To analyze the alterations in gene expression caused by HL156A, RNA was extracted from liver tissues of each experimental group and subjected to RT-qPCR. Among the several ECM components, the mRNA expressions of *col1a1* and *col3a1* were drastically increased by up to 10-fold by TAA. Co-treatment with HL156A reduced *col3a1* levels by up to 60% and those of *col1a1* by up to 30% at either 2 mg/kg or 10 mg/kg dose (Fig. 2A and B). Of note, the mRNA level of tgf-β1, a potent profibrogenic factor was also significantly decreased by HL156A co-treatment (Fig. 2C).

*TAA-induced HSC activation and endothelial capillarization are reversed by HL156A*. One major feature of hepatic fibrosis is the activation of hepatic stellate cells, which is characterized by the expression of myofibroblast markers such as α-SMA and desmin. To address cellular events regulated by HL156A, we analyzed liver histology using myofibroblast markers. As shown earlier, TAA administration led to upregulation of α-SMA- as well as desmin-positive cell populations (Fig. 3A). HL156A significantly and dose-dependently diminished both α-SMA and desmin-positive immunoreactivity (Fig. 3A-C). These results indicate that HL156A inhibits HSC activation, which is a critical step in hepatic fibrogenesis.

Several lines of evidence revealed that liver sinusoidal endothelium underwent vascular remodeling upon fibrogenesis (6,22). The loss of liver sinusoid characteristics, referred to as capillarization, is known to accelerate HSC activation (7). As previously reported (23), we observed an increase in

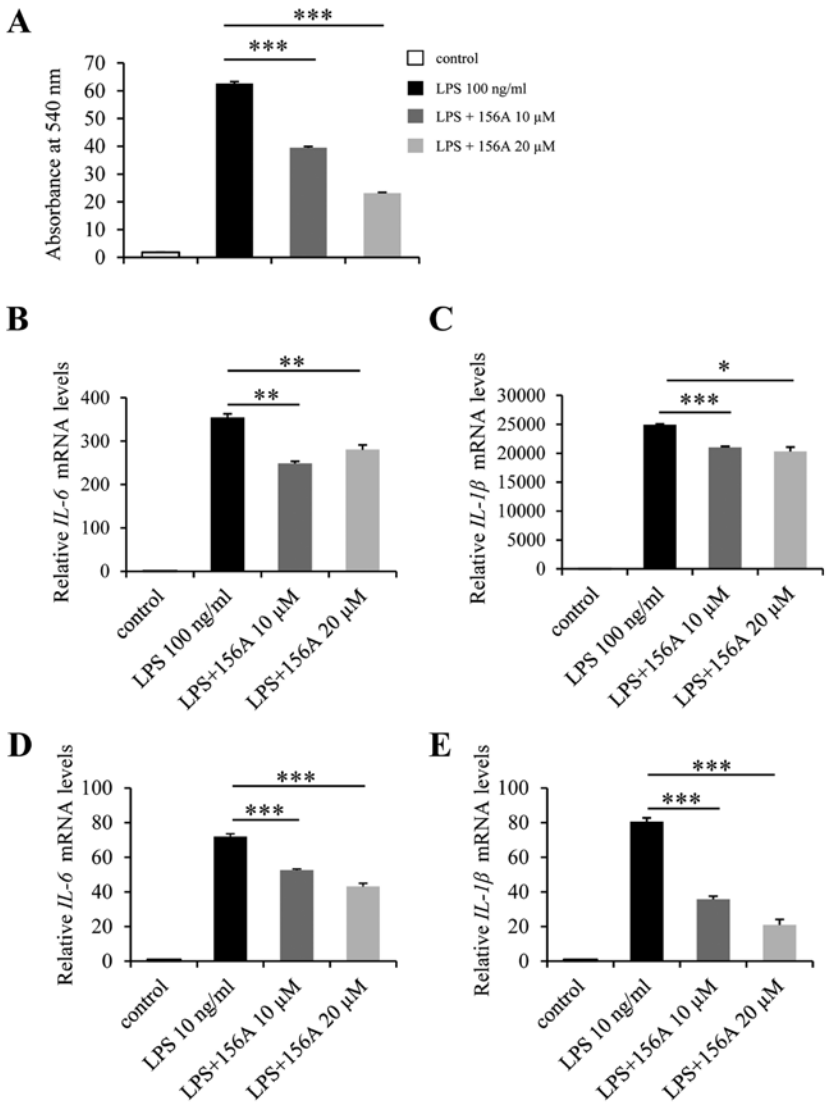


Figure 5. HL156A reduces macrophage inflammation induced by LPS. (A) NO production was measured from the conditioned media of Raw264.7 macrophage cell line. Cells were treated with LPS alone or in combinations of indicated doses of HL156A for 24 h. (B-C) RT-qPCR was performed in Raw264.7 cells treated with LPS alone or in combination of HL156A for 4 h. Note that LPS greatly increases IL-6 (B) and IL-1β (C) mRNA expressions and HL156A partially decreases LPS-induced IL-6 (B) and IL-1β (C) productions. Primary macrophages were cultured with LPS alone or in combination of HL156A for 4 h and relative mRNA levels of IL-6 (D) or IL-1β (E) were quantified by RT-qPCR. Co-treatment of LPS and HL156A reduced both IL-6 (D) and IL-1β (E) levels induced by LPS. Values are relative to control group normalized by GAPDH levels (n=3). Error bars indicate SEM. $^{*}$P<0.05, $^{**}$P<0.01, $^{***}$P<0.001.

laminin-positive area in close proximity to fibrosis area in the liver sections of TAA treated animals (Fig. 3A). High dose of HL156A (10 mg/kg) significantly reduced laminin area while there was no significant reduction in the laminin immunoreactivity at low doses of HL156A (2 mg/kg).

*HL156A attenuates TGF-β1-mediated HSC activation via the activation of AMPK*. To further study the anti-fibrotic effect of HL156A *in vitro*, we took advantage of the rat HSC cell line HSC-T6. MTS assay was carried out to determine proper doses of HL156A without cytotoxicity. HSC-T6 cells were treated with serial doses of HL156A ranging from 1 to 100 $\mu$M for 24 h and relative cell viabilities were measured. As shown in Fig. 4A, no significant cytotoxicity was observed up to 20 $\mu$M while HL156A concentrations over 50 $\mu$M showed some cytotoxicity. Preliminary experiments revealed that there is no or limited effect of HL156A on TGF-β1-induced HSC activation at concentrations <10 $\mu$M (data not shown). The treatment of HSC-T6 cells with TGF-β1 resulted in induction of α-SMA; simultaneous treatment with HL156A attenuated TGF-β1-mediated α-SMA induction at doses of 10 to 20 $\mu$M (Fig. 4B). Since HL156A is a new AMPK activator, we next investigated whether or not the inhibitory effect of HL156A on HSC activation involved AMPK activation. Treatment with HL156A promoted AMPK phosphorylation in a dose-dependent manner, whereas Smad phosphorylation by TGF-β1 was not affected by HL156A (Fig. 4C). Moreover, the inhibitory effect of HL156A on α-SMA expression was reversed by co-treatment with the AMPK inhibitor, compound C (Fig. D). These data revealed that HL156A has an inhibitory effect on HSC activation, probably via the stimulation of AMPK signaling.

*HL156A diminishes LPS-induced macrophage activation*. Inflammation is closely associated with liver fibrosis (3) and there are several studies reporting protective effects of

AMPK signaling in inflammation (11,16). To examine the anti-inflammatory effect of HL156A, LPS, a potent proinflammatory agent was added to Raw264.7 cell culture, which is a widely used mouse macrophage cell line. As expected, LPS treatment of Raw264.7 cells increased the production and release of NO by up to 60-fold. This LPS-induced NO release was diminished by HL156A in a dose-dependent manner (Fig. 5A). We next examined if HL156A was capable of regulating proinflammatory cytokines. Raw264.7 cells were treated with LPS for 4 h with or without HL156A, and the relative mRNA levels of proinflammatory cytokines were analyzed. A single treatment of inactivated Raw264.7 cells with LPS resulted in up to 350-fold increase in IL-6 and 25,000-fold increase in IL-1β transcripts. However, HL156A decreased the levels of IL-6 and IL-1β transcripts by approximately 30 and 20%, respectively (Fig. 5B and C). The inhibitory effect of HL156A on LPS-induced inflammation was further confirmed in primary macrophages, which were isolated and differentiated from mouse bone marrow. HL156A reduced the levels of both IL-6 and IL-1β mRNA in primary macrophages also and more efficiently than in Raw264.7 cells (Fig. 5D and E). Together, these results demonstrate that HL156A inhibits inflammation, which is probably responsible for its anti-fibrotic activity, at least in part.

## Discussion

In the present study, we demonstrate the potential therapeutic effect of a novel AMPK activator, HL156A, in hepatic fibrosis. We found that HL156A inhibited TAA-induced liver fibrosis in mice. Specifically, it reduced ECM deposition and TGF-β1 expression, which are induced by TAA administration. Histological analysis also revealed that the activation of HSCs and capillarization of LSECs are diminished by HL156A. *In vitro* experiments using rat HSC cell line and cultured macrophages further confirmed the inhibitory effects of HL156A on both TGF-β1-induced HSC activation and LPS-induced inflammation of macrophages. As AMPK is expressed ubiquitously in almost all cells and organs, HL156A seems to target multiple cell types in inhibiting hepatic fibrosis. Our results also imply that HL156A may affect multiple responses to fibrotic insult such as inflammation, capillarization of LSECs, and myofibroblastic transition of HSCs. However, since these multiple responses influence each other, further studies would be needed to figure out the exact point of action of HL156A in *in vivo* settings.

Fibrosis is a wound healing response that can be considered as a part of innate immunity. Therefore, multiple organs including the liver, lung, kidney, and peritoneum commonly develop fibrosis upon chronic tissue injuries (24). There are common molecular mechanisms involved in fibrosis of multiple organs such as αv integrin and TGF-β signaling pathways (25,26). In this context, it is noteworthy that HL156A has been recently reported to show inhibitory effects in peritoneal fibrosis. In light of the results of our present work on liver fibrosis and previous ones on peritoneal fibrosis (18), it would be worthwhile to explore the anti-fibrotic effects of HL156A in other organ systems such as pulmonary fibrosis and renal fibrosis to determine whether HL156A can be developed as an anti-fibrosis drug targeting multiple organs.

Since metabolic derangement is considered as one of the major causes of many human cancers, the pharmacological activators of AMPK are being revisited for cancer therapy (27). The importance of metabolic dysregulation in liver cancer has been studied extensively. The components of the AMPK signaling pathway, likely, play a crucial role in hepatocellular carcinogenesis (28-30). Among organs that develop fibrosis, the liver is the one in which fibrosis is the most closely associated with cancer (31). Approximately 90% of hepatocellular carcinoma (HCC) cases arise in cirrhotic livers (32) and the incidence of HCC is approximately 15% in HBV patients with cirrhosis (33). Thus, targeting liver fibrosis and HCC simultaneously would be an efficient strategy rather than treating either fibrosis or HCC in isolation. HL156A, as an AMPK activator with an anti-fibrotic effect, may benefit the development of new strategies targeting liver cancer with cirrhosis.

## Acknowledgements

This work was supported by the Global Research Laboratory Program (2011-0021874), the Global Core Research Center (GCRC) Program (2011-0030001) through the National Research Foundation (NRF) funded by the Korean Ministry of Science, ICT and Future Planning (MSIP), and the NRF grant funded by the Korea government (MSIP) (2015R1C1A2A01054446).

## References

1. Lee SJ, Kim KH and Park KK: Mechanisms of fibrogenesis in liver cirrhosis: The molecular aspects of epithelial-mesenchymal transition. World J Hepatol 6: 207-216, 2014.
2. Seki E and Schwabe RF: Hepatic inflammation and fibrosis: Functional links and key pathways. Hepatology 61: 1066-1079, 2015.
3. Pellicoro A, Ramachandran P, Iredale JP and Fallowfield JA: Liver fibrosis and repair: Immune regulation of wound healing in a solid organ. Nat Rev Immunol 14: 181-194, 2014.
4. Friedman SL: Mechanisms of hepatic fibrogenesis. Gastroenterology 134: 1655-1669, 2008.
5. Bataller R and Brenner DA: Liver fibrosis. J Clin Invest 115: 209-218, 2005.
6. Iwakiri Y, Shah V and Rockey DC: Vascular pathobiology in chronic liver disease and cirrhosis - current status and future directions. J Hepatol 61: 912-924, 2014.
7. Langer DA, Das A, Semela D, Kang-Decker N, Hendrickson H, Bronk SF, Katusic ZS, Gores GJ and Shah VH: Nitric oxide promotes caspase-independent hepatic stellate cell apoptosis through the generation of reactive oxygen species. Hepatology 47: 1983-1993, 2008.
8. Deleve LD, Wang X and Guo Y: Sinusoidal endothelial cells prevent rat stellate cell activation and promote reversion to quiescence. Hepatology 48: 920-930, 2008.
9. Grahame Hardie D: Regulation of AMP-activated protein kinase by natural and synthetic activators. Acta Pharm Sin B 6: 1-19, 2016.
10. Vallianou NG, Evangelopoulos A and Kazazis C: Metformin and cancer. Rev Diabet Stud 10: 228-235, 2013.
11. Salt IP and Palmer TM: Exploiting the anti-inflammatory effects of AMP-activated protein kinase activation. Expert Opin Investig Drugs 21: 1155-1167, 2012.
12. Salminen A, Kaarniranta K, Haapasalo A, Soininen H and Hiltunen M: AMP-activated protein kinase: A potential player in Alzheimer's disease. J Neurochem 118: 460-474, 2011.
13. Li J, Pan Y, Kan M, Xiao X, Wang Y, Guan F, Zhang X and Chen L: Hepatoprotective effects of berberine on liver fibrosis via activation of AMP-activated protein kinase. Life Sci 98: 24-30, 2014.
14. Tripathi DM, Erice E, Lafoz E, García-Calderó H, Sarin SK, Bosch J, Gracia-Sancho J and García-Pagán JC: Metformin reduces hepatic resistance and portal pressure in cirrhotic rats. Am J Physiol Gastrointest Liver Physiol 309: G301-G309, 2015.

15. Lim JY, Oh MA, Kim WH, Sohn HY and Park SI: AMP-activated protein kinase inhibits TGF-β-induced fibrogenic responses of hepatic stellate cells by targeting transcriptional coactivator p300. J Cell Physiol 227: 1081-1089, 2012.
16. Jeong HW, Hsu KC, Lee JW, Ham M, Huh JY, Shin HJ, Kim WS and Kim JB: Berberine suppresses proinflammatory responses through AMPK activation in macrophages. Am J Physiol Endocrinol Metab 296: E955-E964, 2009.
17. Guo T, Woo SL, Guo X, Li H, Zheng J, Botchlett R, Liu M, Pei Y, Xu H, Cai Y, *et al*: Berberine ameliorates hepatic steatosis and suppresses liver and adipose tissue inflammation in mice with diet-induced obesity. Sci Rep 6: 22612, 2016.
18. Ju KD, Kim HJ, Tsogbadrakh B, Lee J, Ryu H, Cho EJ, Hwang YH, Kim K, Yang J, Ahn C, *et al*: HL156A, a novel AMP-activated protein kinase activator, is protective against peritoneal fibrosis in an in vivo and in vitro model of peritoneal fibrosis. Am J Physiol Renal Physiol 310: F342-F350, 2016.
19. Mobley AK, Tchaicha JH, Shin J, Hossain MG and McCarty JH: Beta8 integrin regulates neurogenesis and neurovascular homeostasis in the adult brain. J Cell Sci 122: 1842-1851, 2009.
20. Shin MW, Bae SJ, Wee HJ, Lee HJ, Ahn BJ, Le H, Lee EJ, Kim RH, Lee HS, Seo JH, *et al*: Ninjurin1 regulates lipopolysaccharide-induced inflammation through direct binding. Int J Oncol 48: 821-828, 2016.
21. Liu Y, Meyer C, Xu C, Weng H, Hellerbrand C, ten Dijke P and Dooley S: Animal models of chronic liver diseases. Am J Physiol Gastrointest Liver Physiol 304: G449-G468, 2013.
22. DeLeve LD: Liver sinusoidal endothelial cells in hepatic fibrosis. Hepatology 61: 1740-1746, 2015.
23. Straub AC, Stolz DB, Ross MA, Hernández-Zavala A, Soucy NV, Klei LR and Barchowsky A: Arsenic stimulates sinusoidal endothelial cell capillarization and vessel remodeling in mouse liver. Hepatology 45: 205-212, 2007.
24. Rockey DC: Current and future anti-fibrotic therapies for chronic liver disease. Clin Liver Dis 12: 939-962, xi, 2008.
25. Henderson NC, Arnold TD, Katamura Y, Giacomini MM, Rodriguez JD, McCarty JH, Pellicoro A, Raschperger E, Betsholtz C, Ruminski PG, *et al*: Targeting of αv integrin identifies a core molecular pathway that regulates fibrosis in several organs. Nat Med 19: 1617-1624, 2013.
26. Munger JS, Huang X, Kawakatsu H, Griffiths MJ, Dalton SL, Wu J, Pittet JF, Kaminski N, Garat C, Matthay MA, *et al*: The integrin alpha v beta 6 binds and activates latent TGF beta 1: A mechanism for regulating pulmonary inflammation and fibrosis. Cell 96: 319-328, 1999.
27. Kuhajda FP: AMP-activated protein kinase and human cancer: Cancer metabolism revisited. Int J Obes 32 (Suppl 4): S36-S41, 2008.
28. Ferretti AC, Tonucci FM, Hidalgo F, Almada E, Larocca MC and Favre C: AMPK and PKA interaction in the regulation of survival of liver cancer cells subjected to glucose starvation. Oncotarget: Feb 15, 2016 (Epub ahead of print).
29. Park SY, Lee YK, Kim HJ, Park OJ and Kim YM: AMPK interacts with β-catenin in the regulation of hepatocellular carcinoma cell proliferation and survival with selenium treatment. Oncol Rep 35: 1566-1572, 2016.
30. Yang CC, Chang SF, Chao JK, Lai YL, Chang WE, Hsu WH and Kuo WH: Activation of AMP-activated protein kinase attenuates hepatocellular carcinoma cell adhesion stimulated by adipokine resistin. BMC Cancer 14: 112, 2014.
31. Zhang DY and Friedman SL: Fibrosis-dependent mechanisms of hepatocarcinogenesis. Hepatology 56: 769-775, 2012.
32. Seitz HK and Stickel F: Risk factors and mechanisms of hepatocarcinogenesis with special emphasis on alcohol and oxidative stress. Biol Chem 387: 349-360, 2006.
33. Fattovich G, Stroffolini T, Zagni I and Donato F: Hepatocellular carcinoma in cirrhosis: Incidence and risk factors. Gastroenterology 127 (Suppl 1): S35-S50, 2004.